



OPEN

Enhanced cold plasma hydrogenation with glycerol as hydrogen source for production of *trans*-fat-free margarine

Ika Priyanti¹, Doonyapong Wongsawaeng¹✉, Grittima Kongprawes¹, Kanokwan Ngaosuwan², Worapon Kiatkittipong³, Peter Hosemann⁴, Phachirarat Sola⁵ & Suttichai Assabumrungrat^{6,7}

The quest for better nutritious foods has encouraged novel scientific investigations to find *trans*-fat reduction methods. This research proposes an innovative approach for the production of healthier *trans*-fat-free margarine from palm oil by the use of dielectric barrier discharge (DBD) plasma technology with glycerol serving as the principal source of hydrogen. The effectiveness of DBD plasma in hydrogenating palm olein was investigated. By employing a methodical series of experiments and thorough analytical approaches, examination of the saturated fatty acid conversion experienced its iodine value (IV) reduction from 67.16 ± 0.70 to 31.61 ± 1.10 under the optimal process parameters of 1 L min⁻¹ He flow rate, 35 W plasma discharge power, 10 mm gap size, ambient initial temperature, and 12 h reaction time with solid texture. According to the method for producing *trans*-fat-free margarine in the absence of a catalyst and H₂ gas, the hydrogenation rate of the prepared mixture of palm olein-glycerol was remarkably improved; the *trans*-fat content in the produced product was zero; the efficacy of incorporating *cis*- and *trans*-isomerization was lowered, and the method has a promising industrial application prospect.

Keywords Plasma hydrogenation, *Trans*-fat-free margarine, Glycerol, Hydrogen donor

An innovative way to convert glycerol into valuable products is a crucial and promising area of research. Converting glycerol into valuable products helps create a circular economy by turning waste into a resource and solves the glycerol waste disposal problem^{1,2}. Glycerol is commonly known as glycerol alcohol or glycerine. It was discovered in 1779³. As a biodiesel byproduct, it can be utilized as a sustainable source in biofuels, medicines, cosmetics, pharmaceuticals, chemicals, and food industries⁴⁻⁸. Notably, the food business has seen a rise in demand for healthier products. The increased understanding of health risks from *trans*-fats has led to a pursuit of healthier ingredients and production methods. Because of the adverse health effects of *trans*-fats, a recommendation to restrict the consumption of *trans*-fats is issued by The World Health Organization (WHO) and the food and agriculture organization (FAO) of the United Nations. This equates to a daily intake of fewer than 2.2 g for individuals following a 2,000 cal diet⁹. The WHO has also started a global program called REPLACE, which stands for Review, Promote, Legislate, Assess, Raise Awareness, and Enforce. The goal of this program is to get industrially made *trans*-fat out of the world's food supply by 2023¹⁰.

¹Research Unit on Plasma Technology for High-Performance Materials Development, Department of Nuclear Engineering, Faculty of Engineering, Chulalongkorn University, 254 Phayathai Road, Pathum Wan, Bangkok 10330, Thailand. ²Division of Chemical Engineering, Faculty of Engineering, Rajamangala University of Technology Krungthep, Bangkok 10120, Thailand. ³Department of Chemical Engineering, Faculty of Engineering and Industrial Technology, Silpakorn University, Nakhon Pathom 73000, Thailand. ⁴Department of Nuclear Engineering, Faculty of Engineering, University of California at Berkeley, Berkeley, California 94720, USA. ⁵Nuclear Technology Research and Development Center, Thailand Institute of Nuclear Technology (Public Organization), Nakhon Nayok 26120, Thailand. ⁶Center of Excellence in Catalysis and Catalytic Reaction Engineering, Department of Chemical Engineering, Faculty of Engineering, Chulalongkorn University, Bangkok 10330, Thailand. ⁷Bio-Circular-Green-Economy Technology & Engineering Center (BCGeTEC), Faculty of Engineering, Chulalongkorn University, Bangkok 10330, Thailand. ✉email: Doonyapong.W@chula.ac.th

Trans-fats, commonly known as *trans*-fatty acids (TFAs), are usually found in margarine, a popular substitute for butter. Margarines contain 15.2–54.1% of saturated fatty acids, which is less than those in butter. The content of linoleic fatty acid varies between 3.7 and 52.4% in portions of margarine¹¹. TFAs are produced through partial hydrogenation of vegetable oils, and are linked to an increased risk of several comorbidities such as cardiovascular diseases, hepatic damage and brain diseases, the brain and nervous system, depression risk, Alzheimer's disease, and other health complications^{12,13}. The fat of animal products (meat and milk) constitutes an essential source of naturally occurring TFAs; however, the TFAs content in ruminant fat, known as ruminant-produced *trans*-fat (RPTFAs)¹⁴, is considerably lower and may not exceed 6% of total fatty acids (on average 4% of total fatty acid (FA), and sometimes up to 8% of total FA in milk fat)^{15,16}. Specifically, RPTFAs are produced by the bacterial hydrogenation of unsaturated fatty acids in the first stomach of the rumen, such as in cattle, sheep, and goats. The process called biohydrogenation or ruminal biohydrogenation is the process where the bacteria secrete enzymes which convert *cis* fatty acids into *trans* fatty acids through certain pathways¹⁷.

In the pursuit of innovative and sustainable solutions, plasma technology has risen as a promising method for converting palm olein into healthier margarine. The ability of dielectric barrier discharge (DBD) plasma, a non-thermal plasma technique, to efficiently modify complex molecular structures without excessive heat generation has attracted considerable interest. DBD plasma is therefore an ideal candidate to produce *trans*-fat-free margarine, as it facilitates the selective hydrogenation of unsaturated fatty acids without the introduction of harmful *trans*-fats especially when coupled with optimized plasma parameters and processing conditions¹⁸. *Trans*-fat-free margarine by cold plasma hydrogenation has been investigated in previous studies^{19–21}, and hydrogen gas was used as a hydrogen source. Meanwhile, the production cost needed to be reduced when this technology was to be industrially scaled up. Palm olein is widely available globally, making it accessible to food manufacturers and processors in various regions. It is derived from palm oil and is naturally rich in unsaturated fatty acids, particularly oleic acid and linoleic acid. This high degree of unsaturation makes it an excellent starting material for hydrogenation because it can be selectively saturated to achieve desired levels of saturation.

Finding a suitable hydrogen donor to facilitate the conversion of unsaturated fatty acids into healthful saturated fatty acids is the most challenging aspect of this process. Glycerol has emerged as a promising candidate for this function due to the presence of numerous hydroxyl groups in glycerol molecules, making it a potential hydrogen source that can neutralize the double bonds in unsaturated fatty acids via plasma-induced reactions. In plasma containing helium gas, glycerol acts as a hydrogen donor through the decomposition/cracking reaction, $C_3H_8O_3 \rightarrow 3CO + 4H_2$ ^{6,22}. When the hydrogen plasma is in contact with the oil, the gas/plasma-liquid interaction directly triggers a reaction in the bulk of the oil. The formation of high-energy electrons, ions, and radicals has potential pathways to transform unsaturated fat into saturated fat with low or even free *trans*-fat^{23–25}. Therefore, the possibility of using glycerol, as with other alcohols, as an environmentally friendly donor solvent in transfer hydrogenation–dehydrogenation reactions was explored²⁶.

This study seeks to determine the viability and effectiveness of producing *trans*-fat-free margarine from palm oil using DBD plasma technology and glycerol as a hydrogen donor without any catalyst. The aims are to optimize the conversion of unsaturated fatty acids, improve the nutritional profile of the final product, and reduce harmful *trans*-fats to negligible levels by analyzing the impact of process parameters and reaction conditions. This research is significant not only because it offers a healthier alternative to conventional margarine, but also because it utilizes the potential of DBD plasma technology for food industrial applications. Several studies in plasma technology have been performed to reduce microbial count, pesticides, and allergens in food products^{27–29}. The growth of DBD is incorporated into the food industry due to its low costs at the industrial scale³⁰. Meanwhile, due to its configuration and flexibility for the electrode shape and the dielectric material used, this technology has become the most convenient form of plasma generation³⁰. In addition, the use of glycerol as a hydrogen donor can provide a sustainable solution for managing the growing surplus of glycerol produced by the biodiesel industry. By presenting a novel and environmentally friendly approach to *trans*-fat-free margarine production through the application of DBD plasma technology, harnessing the hydrogen-donating properties of glycerol, the outcomes of this research are expected to contribute significantly to the food industry.

Materials and methods

Chemicals

Refined palm olein of the Gaysorn brand was obtained from a local supermarket in Bangkok, Thailand, and it was used directly without any pretreatment. Glycerol (99.5%) was purchased from QReC. Ultra-high purity (UHP) He gas distributed by Alternative Chemical Company was used for plasma generation and hydrogenation. The following chemicals were used for the evaluation of iodine value (IV): 0.1N Wij's solution distributed by RCI Labscan and 99.5% cyclohexane distributed by Loba Chemical.

Experimental setup

The plasma reactor setup shown in (Fig. 1) consists of a parallel-type dielectric barrier discharge (DBD) reactor, a neon high-voltage power supply, and a hot plate stirrer. The reactor was made of a Pyrex glass chamber with 2-mm thick aluminum plates as an upper HV electrode and a lower electrode. Both electrodes were 50 mm × 110 mm in dimensions. A 1 mm thick alumina dielectric plate was attached to the bottom of the upper electrode. The lower electrode was placed outside the reactor acting as a ground electrode. The neon high-voltage power supply (HONGBA C-10, Hyrite Lightning Co.) was connected to the electrodes with a fixed frequency of 22 kHz, and provided maximum open-circuit voltage and current output of 10 kV AC and 30 mA, respectively. The plasma discharge power was controlled by a variac connected to the neon power supply. The gas inlet was controlled using a Bronkhorst mass flow controller (error: ± 0.03 mL min⁻¹). A thermometer was placed inside

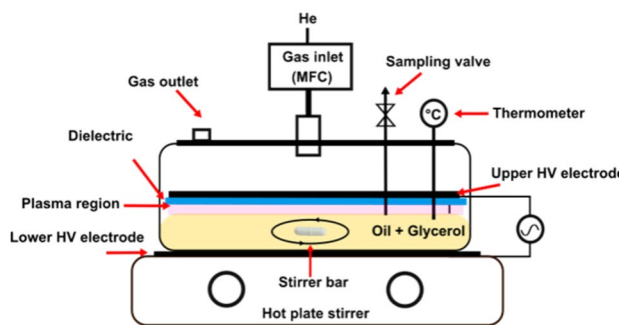


Figure 1. Drawing of the experimental setup.

the chamber to monitor the reaction temperature. The hotplate stirrer was positioned under the reactor to agitate the oil-glycerol mixture for effective mass transfer and to control the temperature if needed.

Plasma hydrogenation of palm olein

Before each experiment, the reactor was continuously purged with 1 L min^{-1} of the carrier gas (He) for 3–5 min to ensure that the system was air-free. Afterward, the gas flow rate was adjusted to the desired level. A desired gap size was adjusted until the appearance of the plasma region. The volume of the oil-glycerol mixture was fixed at 35 mL to allow the mixture to completely cover the bottom of the chamber. The mixed solution was stirred at 200 rpm during the reaction for 2 h of reaction time.

Table 1 presents influential parameters and their respective ranges of investigation. The molar ratio of palm oil to glycerol, a crucial parameter affecting the degree of hydrogenation, was maintained at a baseline of 1:1, and examined within a range of 1:0.5 to 1:5. The gap distance between the upper electrode and the surface of the oil-glycerol mixture, affecting plasma intensity and distribution, was set at 10 mm initially, and was varied from 5 to 15 mm. The flow rate of the plasma-generating gas, influencing the reaction kinetics, was held at 1 L min^{-1} , and was explored between 0.5 and 1 L min^{-1} . The reaction temperature was initially set at room temperature ($27\text{ }^{\circ}\text{C}$) and was investigated within the range of 20 to $50\text{ }^{\circ}\text{C}$ initially. Temperature control was achieved via external cooling or heating. The minimum power to generate plasma with stable glow discharge in the constructed chamber was found to be 35 W at a 10 mm gap size. To investigate the degree of unsaturated fat transformation due to the plasma discharge power variation, the discharge power was varied from 35 to 75 W. The discharge power of 75 W was the maximum that the neon power supply could provide. Lastly, the reaction time was initially set at 2 h, but was also examined further until the semisolid state of the product was obtained. Each experiment was repeated two times for reproducibility purposes.

Emulsification preparation

The homogenization step was conducted using the hotplate stirrer under the reaction chamber. First, edible palm olein and glycerol were accurately measured and poured into the reaction chamber. During the homogenization process, the stirrer was operated at 200 rpm to reduce oil droplet size and achieve uniform distribution of the two compounds throughout the mixture. The use of this method resulted in a finely dispersed oil-glycerol emulsion, leading to a smooth, creamy texture in the final margarine product.

Palm olein, glycerol, and product characterization

Iodine value

Iodine value (IV) measurement was performed based on the previous method by Puprasit et al.¹⁹, and it was measured in duplicates. The sample was weighted at 0.4 g, mixed with 15 mL cyclohexane and 25 mL Wiji's solution, and then left for 1 h. A 20 mL 10% KI solution (w/v) was added to stop the reaction, and 150 mL DI water was poured to dilute. A 5% (w/v) starch solution was prepared to be an indicator of color changes. Sodium

Parameter	Baseline	Range
Oil-to-glycerol molar ratio	1:1	1:0.5–1:5
Gap (mm)	10	5–15
Plasma discharge power (W)	75	35–75
Temperature ($^{\circ}\text{C}$)	Room temperature (27)	Room temperature (27)–50
Flowrate (L min^{-1})	1	0.5–1
Reaction time (h)	2	(or until semisolid)

Table 1. Range of influential process parameters.

thiosulfate ($\text{Na}_2\text{S}_2\text{O}_3$) of 0.1 N was used as a titrant and IV was calculated by Eq. (1). A blank solution was prepared by repeating the previous steps.

$$\text{IV} = \frac{(V_1 - V_2) \times N \times 12.69}{\text{mass of sample (g)}} \quad (1)$$

where V_1 is the volume of $\text{Na}_2\text{S}_2\text{O}_3$ titration in the blank (mL); V_2 is the volume of $\text{Na}_2\text{S}_2\text{O}_3$ titration in the sample (mL); and N is the normality of $\text{Na}_2\text{S}_2\text{O}_3$.

Viscosity

Calculation of mixed-liquid viscosity was performed according to Eq. (2) following the previous method by Arrhenius and Graham's model^{31,32}.

$$\mu_{\text{mix}} = N_1 \cdot \mu_1 + N_2 \cdot \mu_2 \quad (2)$$

where μ_{mix} is the viscosity of the mixed solution (cST); N_1 and μ_1 are the mole fraction and viscosity, respectively, of component 1 (palm olein); N_2 and μ_2 are the mole fraction and viscosity, respectively, of component 2 (glycerol).

ATR-FTIR and GC-MS

Attenuated total reflectance-fourier transform infrared (ATR-FTIR) spectroscopy was utilized to obtain qualitative data on the product samples, with the sample preparation described by Amorim et al.³³. Before data acquisition, the sample (semisolid/liquid form) was heated at 50 °C in the vial until melting, and 10 μL of the melted fat was used for each analysis. FTIR spectra were recorded using the Bruker ATR-FTIR spectrometer (Bruker Corporation, Massachusetts, U.S.A.) in the middle infrared mode equipped with an ATR sampling device. Spectra were acquired within a wavenumber range of 4000–650 cm^{-1} with 16 scans at 4 cm^{-1} resolution.

The fatty acid compositions were determined by gas chromatography-mass spectrometry (GC-MS). The results were presented as percent compositions of several fatty acid profiles of the feed palm olein and hydrogenated palm olein-glycerol. It also provided a percentage content of *cis*- and *trans*-isomers.

Optical emission spectroscopy

The plasma emission spectra were scanned using a high-resolution spectrometer (Ocean Optics, model HR2000+) equipped with a 1,200 μm optical fiber in the range of 200–1,100 nm with an OceanView version 2.0.8 software to monitor UV, VIS, and IR wavelengths. The distance between the optical fiber and the plasma chamber was 50 mm. The OES spectra were corrected for background noise. The NIST Atomic Spectra Database was used to identify the OES peaks following the procedure of the previous report²⁵.

Acid value (AV), slip melting point (SMP), spreadability, and hardness test

The assessment of acid value (AV) adhered to the guidelines outlined by IUPAC 1987¹⁹. This involved combining a 2 g sample with 25 mL of diethyl ether and 25 mL of 95% ethanol, followed by the addition of 0.5 mL of 0.1% phenolphthalein solution. Titration was then conducted using a 0.1 M potassium hydroxide solution. The AV can be determined using the formula: $\text{AV} = (V \times 5.16)/W$, where V represents the volume of the potassium hydroxide solution and W denotes the weight of the sample.

The AOCS official method CC 3-25 was used to determine the slip melting point (SMP) with an open-ended capillary tube²¹. The SMP was measured three times to validate the presence of statistical error.

The textural analysis of the products; i.e., spreadability and hardness, was performed using the INSTRON 5943 in compression mode. The hardness test method followed the previous investigation by Puprasit et al.¹⁹ using a speed of 13 mm min^{-1} , a load capacity of 100 N, and a temperature of 25 ± 1 °C. The spreadability test followed the previous work proposed by Wongjaikham et al.²¹ utilizing male and female 45° cone probes, which involved the material to a temperature of 25 ± 1 °C. The male cone was inserted into the sample within the female cone, maintaining 13 mm, a load capacity of 100 N, and moving at a speed of 1 mm s^{-1} . The sample was assessed four times for reproducible statistical error. The spreadability can be determined by calculating the area under the positive peak.

Results and discussion

Influence of oil-to-glycerol molar ratio

The IV measurement helps determine the conversion of unsaturated fat into saturated fat. An increase in saturated fat indicates a more successful breakdown of C=C double bonds in palm olein during hydrogenation. An investigation on the glycerol ratio was conducted to check the decrease in IV which indicates the degree of hydrogenation. Investigations started with four variations of oil-to-glycerol molar ratio between 1:0.5, 1:1, 1:3, and 1:5. The total volume of the solution was fixed at 35 mL. The reaction was set with a gap size of 10 mm, 1 L min^{-1} He gas flow rate, 75 W of plasma discharge power, ambient temperature with an initial temperature of 27 °C, and stirring rate of 200 rpm for 2 h of reaction time. The influence of the oil-to-glycerol molar ratio on IV is shown in (Fig. 2). The feed referred to the refined palm olein oil fed into the reactor without glycerol mixed before plasma treatment. This was set as a control with the IV of 67.16 ± 0.70 . The finding was that the IV of the molar ratio of 1:1 decreased the most from the initial feed value to 42.85 ± 4.84 . For the ratios of 1:0.5, 1:3, and 1:5, the IV increased from the ratio of 1:1.

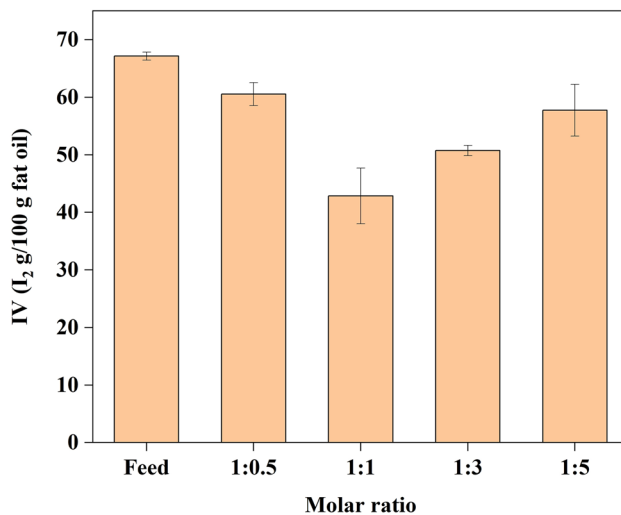


Figure 2. IV of oil in the investigation of oil-to-glycerol molar ratio (10 mm gap size, 1 L min⁻¹ He gas flow rate, 75 W plasma discharge power, ambient temperature with initial temperature of 27 °C, and 2 h of reaction time).

A high glycerol content resulted in a high mixed viscosity. This was supported by the calculation proposed by Arrhenius' and Graham's model^{31,32}, with the expression for the viscosity of a mixed solution highlighted in Sect. "Viscosity". The calculated viscosity of each molar ratio is shown in (Table 2).

When the ratio of 1:0.5 was applied, low viscosity allowed the mixed solution to move easily in the reaction chamber, enabling a thorough reaction with the plasma. However, due to the small amount of hydrogen source, IV only decreased by about 7 points from the feed value. When the ratio increased to 1:1, this condition seemed to match Kongprawes et al.'s collision hypothesis³⁷, as proper glycerol content in a mixed liquid increased the probability of successful collisions between reactive species in plasma and glycerol molecules, resulting in hydrogen radicals (H) formation through dehydrogenation reaction. The radicals might then contribute to the C=C bonds in the oil molecules becoming single bonds.

The large amount of glycerol from plasma dehydrogenation might produce H radicals very effectively. However, when higher molar ratios of 1:3 and 1:5 were applied, the higher viscosity may potentially disrupt the reaction by slowing down molecular movement and reducing the frequency of collisions between reactant molecules in the reaction chamber, leading to a decrease in reaction rate or even inhibit the interaction between the plasma-liquid surface/interface altogether. Then, the generated H radicals appear to have a challenging circumstance when interacting with the oil. In agreement with Al-Moameri et al.³⁸, it was concluded that increased viscosity leads to a substantial decrease in diffusion rates and, subsequently, reaction rates, resulting in a slow reaction. Since the ratio 1:1 showed the optimal condition in this case, it was consequently fixed to investigate other parameters.

Influence of gap size

To investigate the influence of the gap size, it was varied from 5 to 15 mm. The reaction took place at a 1:1 molar ratio of oil to glycerol, 1 L min⁻¹ He gas flow rate, 75 W of plasma discharge power, ambient temperature with an initial temperature of 27 °C, and stirring rate of 200 rpm for 2 h of reaction time. The obtained results are demonstrated in (Fig. 3). The smallest gap (5 mm) offered the reduction of IV from the initial value of 67.16 ± 0.70 to 53.58 ± 3.48 , and it further reduced to 42.85 ± 4.84 for the 10 mm gap. However, for the larger gap of 15 mm, the IV increased to 57.09 ± 2.66 . It was found that a 10 mm gap offered the most optimal IV reduction.

Molar ratio	Mixed viscosity (g)	IV (I_2 g/100 g fat oil)
1:0	86.97	67.16 ± 0.70
1:0.5	367.48	60.55 ± 1.99
1:1	515.99	42.85 ± 4.84
1:3	734.13	50.76 ± 0.90
1:5	803.81	57.74 ± 4.49

Table 2. Calculated viscosity of mixed solution for each molar ratio of oil to glycerol. *Calculation of each viscosity at room temperature (27 °C, IUPAC standard)³⁴. (1) Palm olein: 86.97 cST (27°C)³⁵. (2) Pure glycerol: 945 cST (27°C)³⁶.

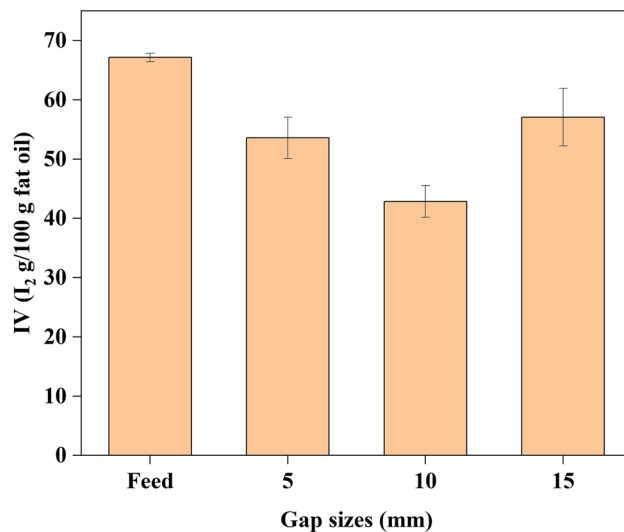


Figure 3. IV of oil in the investigation of gap size (1:1 oil-to-glycerol molar ratio, 1 L min⁻¹ He gas flow rate, 75 W plasma discharge power, ambient temperature with initial temperature of 27 °C, and 2 h of reaction time).

The atmospheric-pressure plasma discharge system was sensitive to the discharge gap distance. As the smallest and largest electrode gaps were constructed in this study, which were 5 and 15 mm, an insufficient or excessive distance separating the two barriers could potentially result in the instability of the gas layer and liquid surface located between them³⁹, resulting in ineffective reduction of IV. A high discharge current, more streamers, as well as more active species, were formed because of the strengthened electric field of 1.01 kV/mm for the 5-mm case. In contrast, a small discharge current was obtained because of the weakened electric field (0.31 kV/mm), showing fewer active species formed for the 15 mm case (see Supplementary Data Table S1).

The increased plasma current in the small gap (5 mm) can enhance the mutual interaction between the plasma and the facing liquid⁴⁰. Nonetheless, impurities such as carbon residue from the burned oil vapor were formed and observed on the upper electrode when the gap size was too small, resulting in decreased plasma performance due to the impact of mutual interactions as illustrated in the previous research (Fig. 4). These impurities were present due to the limited space of active species formed in the plasma while the plasma intensity was increased by the smaller gap size¹⁹. Yoon et al.⁴⁰ proposed the mutual interaction process between plasma and liquid in plasma-treated water (PTW). It was suggested that the conductivity of the PTW became higher after the concentration of the plasma column caused the discharge current to be higher. Then, PTW with higher conductivity increased the discharge current again as the feedback result. This process will cause an abnormal plasma discharge to transit from glow to arc. Similar phenomena of plasma interaction with liquid oil might be experienced with the same characteristics. The transition into the abnormal plasma discharge thus led to the non-uniform discharge, resulting in plasma active species and radicals only interacting with several spots of liquid oil. Due to higher plasma density of these spots, oil and carbon impurities may form on the upper electrode, and the impurities may reduce the efficiency of hydrogenation as was found in the IV reduction of (Fig. 3).

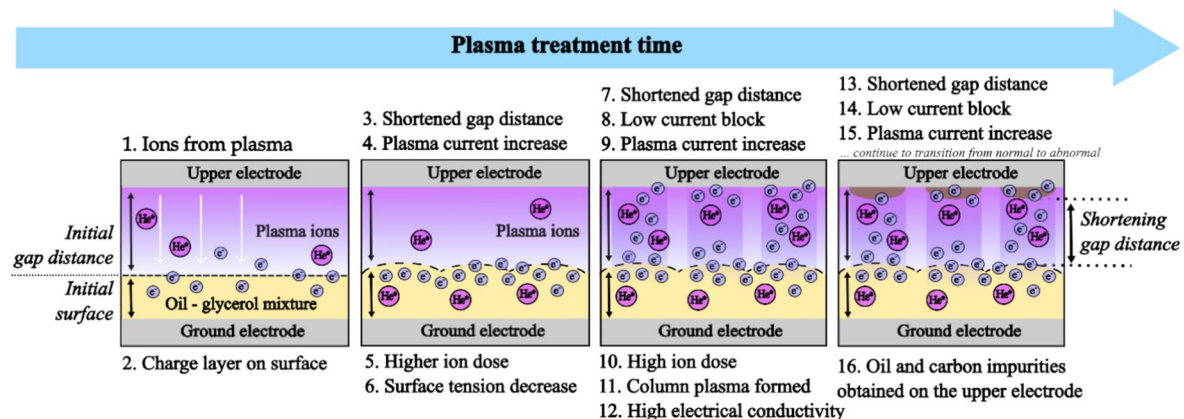


Figure 4. Mutual interaction between plasma and liquid (modified from Yoon et al.⁴⁰).

Conversely, the decreased plasma current and weakened electric field in the wide gap (15 mm) resulted in less effective ionization and excitation of plasma carrier gas⁴¹. It automatically reduced the production of reactive species, such as radicals, which were insufficient to interact with oil and glycerol. As reactive species have more space to diffuse, the longer the travel distances, the more chance of these species undergoing recombination before they can participate in the desired hydrogenation reactions. This results in a lower concentration of reactive species at the reaction site, reducing the overall reactivity and then diminishing the efficiency of hydrogenation. Therefore, a suitable electrode distance is critical. As shown in Fig. 3, the optimal gap size was fixed at 10 mm to investigate the next parameters.

Influence of plasma discharge power

The plasma discharge power was varied at 35, 50, and 75 W at the reaction condition of 1:1 molar ratio of oil to glycerol, gap size of 10 mm, ambient temperature with an initial temperature of 27 °C, 1 L min⁻¹ He gas flow rate, and stirring rate of 200 rpm for 2 h. The results shown in Fig. 5 indicate that 75 W achieved the highest conversion rate of up to 36.2% for unsaturated fatty acids (67.16 ± 0.70 to 42.85 ± 4.84), while conversions at 35 and 50 W were comparatively lower at 15.7% (67.16 ± 0.70 to 56.61 ± 1.81) and 26.8% (67.16 ± 0.70 to 49.19 ± 1.85), respectively. The diminished yield observed at low power may be attributed to the relatively lower energy levels of excited helium, resulting in weaker chemical bond cleavage⁴². The limited formation of excited helium species at low power hindered the conversion of glycerol molecules into hydrogen atoms due to electron energy distribution⁴³. A small fraction of the energetic electrons' distribution might occur due to collisional quenching at atmospheric pressure plasma. Consequently, a significant number of charged particles and excited helium atoms can be lost due to this phenomenon⁴⁴. Conversely, the broader spectrum of excited states at higher discharge power (75 W) provided a wider range of energy options, facilitating a more diverse set of reactions.

Helium exceeds the energy of 24.6 eV with its highest-energy excited state²³. The higher plasma power offered the greater dissociation of He gas, leading to a higher concentration of reactive species in the system to collide with the glycerol molecules to generate hydrogen radicals. To extract hydrogen, the estimation of C-H bonds dissociation energy (BDE) within the hydroxyl groups in glycerol compounds ranges from approximately 350 to 450 kJ/mol which equals 2.19 to 2.81 eV⁴⁵. The surface discharge on the liquid surface typically exhibits an electron density of approximately on the order of 10^{16} cm⁻³ and electron energy > 10 eV²³. These energies are more than sufficient to break down this bond in the plasma-liquid interaction. From the mechanisms of the hydrogenation activity, it was reported that the energy of the C=C double bond was ~ 6.36 eV²³. Afterward, the sum of metastable helium and electron energy levels (> 24.6 eV) can drive H radical with the C=C bond to become a stable single bond³⁷.

Influence of reaction temperature

The effect of initial reaction temperature was investigated at 20 (low-temperature case), 27 (ambient temperature case), and 50 °C (high-temperature case). The plasma power was tuned at 75 W at the reaction condition of 1:1 molar ratio of oil to glycerol, 10 mm gap size, 1 L min⁻¹ He gas flow rate, and stirring rate of 200 rpm for 2 h. For the cooling system, two peristaltic pumps were installed to deliver chilled water circulation surrounding the plasma chamber. For the heating system, external heating from the hot plate stirrer was utilized. Figure 6 presents the temperature history of the mixture during hydrogenation. For the low-temperature case, the steady-state temperature of about 50 °C was reached. For the ambient temperature case, the steady-state temperature of about 80 °C was obtained. For the high-temperature case, the steady-state condition of about 120 °C was reached.

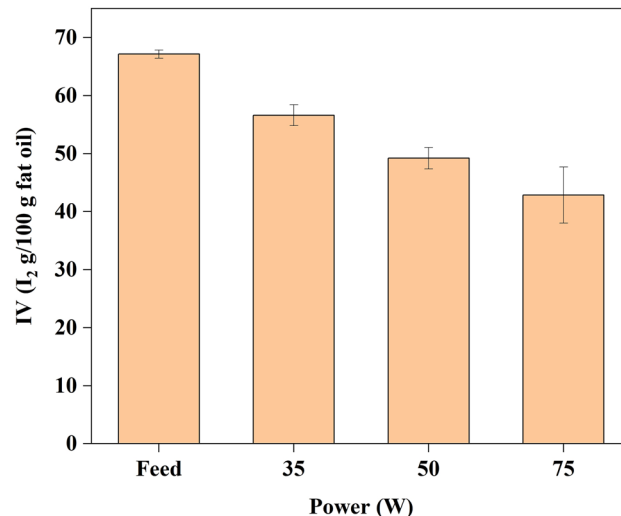


Figure 5. IV of oil in the investigation of plasma discharge power (1:1 oil-to-glycerol molar ratio, 10 mm gap size, 1 L min⁻¹ He gas flow rate, ambient temperature with initial temperature of 27 °C, and 2 h of reaction time).

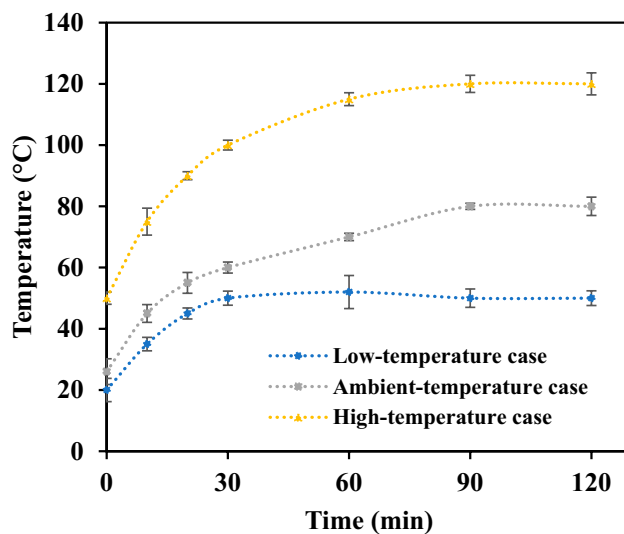


Figure 6. Temperature history from external cooling, ambient, and external heating conditions.

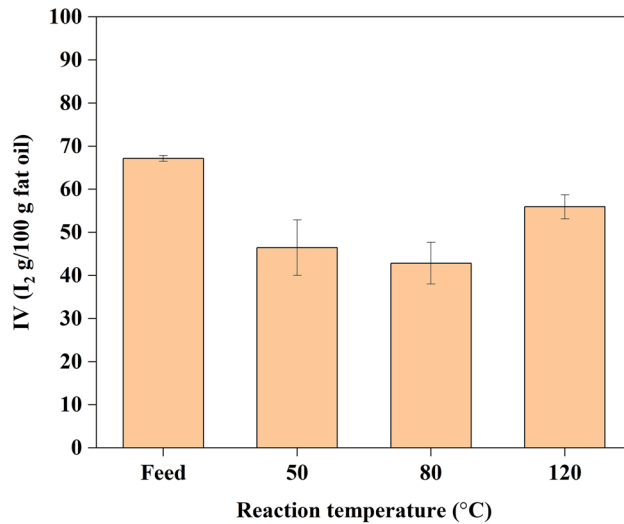


Figure 7. IV of oil in investigation of reaction temperature (1:1 oil-to-glycerol molar ratio, 10 mm gap size, 1 L min⁻¹ He gas flow rate, 75 W plasma discharge power, and 2 h of reaction time).

Figure 7 presents the IV of the oil-glycerol mixture. It was found that the low-temperature condition reduced the IV from 67.16 ± 0.70 to 46.44 ± 6.42 . For the ambient temperature investigation, the largest IV reduction to 42.85 ± 4.84 was achieved. The cooler environment makes the oil more viscous (27.06 cST at 50 °C and 11.61 cST at 80 °C)^{19,20}, making physical interchange between the oil underneath and at the surface layer more difficult. Plasma hydrogenation only occurred at the oil surface; hence, mass transfer limited the reaction. For the high-temperature case, the IV was reduced to only 55.93 ± 2.79 . This aligns with the basic principle that an exothermic reaction should be conducted at a reduced temperature to promote the continuation of the reaction¹⁹. In conclusion, performing the experiment at ambient temperature (initially) without any external heating or cooling yielded the most favorable result, offering the simplest experimental configuration.

Influence of He gas flow rate

To examine the influence of carrier gas flow rate on the reduction of IV, variations of the He flow rate were conducted at 0.8, 1, and 1.5 L min⁻¹. The lowest flow rate was 0.8 L min⁻¹ because it generated a stable plasma. The reaction took place at a 1:1 molar ratio of oil to glycerol, fixed gap size of 10 mm, 75 W of plasma discharge power, ambient temperature with an initial temperature of 27 °C, and stirring rate of 200 rpm for 2 h of reaction time. The obtained results are presented in (Fig. 8). For the cases with 0.8, 1, and 1.5 L min⁻¹, the IV reduction was from 67.16 ± 0.70 to 54.30 ± 0.99 , 42.85 ± 4.84 , and 57.24 ± 0.28 , respectively. The IV reduction of the 1 L min⁻¹

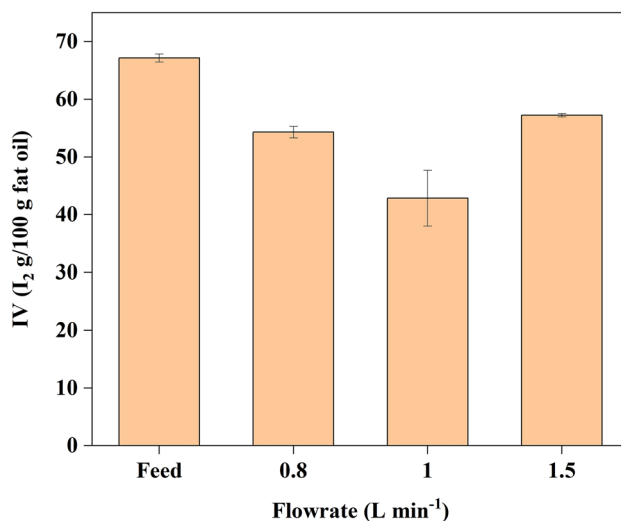


Figure 8. IV of oil in the investigation of He gas flow rate (1:1 oil-to-glycerol molar ratio, 10 mm gap size, 75 W plasma discharge power, ambient temperature with initial temperature of 27 °C, and 2 h of reaction time).

scenario was optimal, with the hydrogenation rate calculated to be 24.31 IV units/120 min or 12.15 IV units/h. Using 0.8 and 1.5 L min⁻¹, the hydrogenation rates were 6.41 and 4.96 IV units/h, respectively.

Owing to this system being in semi-batch operation, the He gas was continuously fed into and withdrawn from the system while the liquid mixture of glycerol and oil was installed in the chamber. The helium flow rate might represent the number of the reactive species generated in the plasma. The gas was associated with helium atoms and ions near the substrate surface during plasma treatment. The extraction of hydrogen atoms from glycerol molecules was initiated by the highly energetic electrons and He^{*} for further adsorption on the material being hydrogenated³⁷.

Therefore, the hydrogenation rate occurring less at a lower flow rate of 0.8 L min⁻¹ might be attributed to a smaller number of reactive species. A higher flow rate of 1.5 L min⁻¹ induced high intensity of reactive species to give rise to the recombination of reactive species to lower the chance of hydrogen atom extraction from glycerol while minimizing the extent of conversion to the desired hydrogenation. It was also suggested that a higher flow rate than 1.5 L min⁻¹ was not preferable due to the increasing cost of reactions/process. The reactant temperature history for each flow rate was illustrated in (Fig. 9) to support this hypothesis.

For the optimal flow rate of 1 L min⁻¹, the system reached its steady-state temperature of 120 °C within the first 15 min. This rapid stabilization resulted from a rising slope of 8 °C/min to the steady-state value. In contrast, the gas flow rates of 0.8 and 1.5 L min⁻¹ exhibited lower slopes of 3.12 and 2.16 °C /min, respectively. The faster temperature ramp rate indicated a higher rate of exothermic hydrogenation as derived from heat released from the system. This assisted in verifying that 1 L min⁻¹ was the most suitable condition. These findings strongly suggested a successful conversion of unsaturated fatty acids into more saturated forms due to the favourable reaction rate.

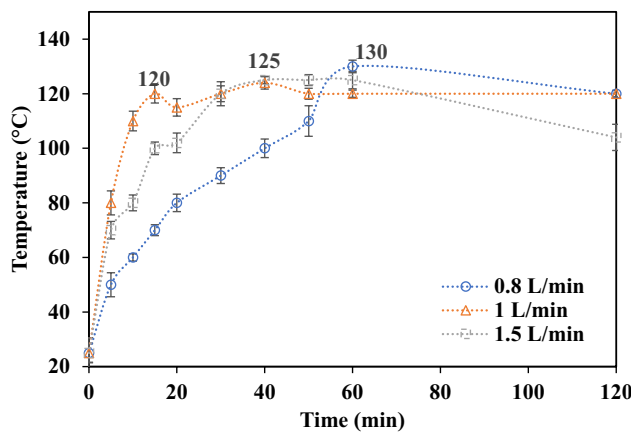


Figure 9. The mixture temperature history of oil-glycerol mixture under different He flow rates.

Influence of reaction time

This study investigated the effect of reaction time, up to 12 h, on the conversion of unsaturated fatty acids into saturated forms, shedding light on the process kinetics. The other process parameters were a 1:1 molar ratio of oil to glycerol, 10 mm gap size, 75 W plasma discharge power, ambient temperature with an initial temperature of 27 °C, 1 L min⁻¹ He gas flow rate, and stirring rate of 200 rpm. The result of IV over the reaction time is presented in (Fig. 10a). The IV decreased from 67.16 ± 0.70 to 42.85 ± 4.84 with a 2 h reaction time, indicating that the fatty acid chains became more saturated. At 4 and 6 h of hydrogenation with IV of 38.65 ± 0.95 and 34.23 ± 1.31, the color of the hydrogenated oil-glycerol mixture with semisolid emulsion particles became paler. At 12 h of reaction time with the IV of 34.05 ± 1.54, the mixture became very viscous as presented in (Fig. 10b). The samples in the Eppendorf tubes were placed upside-down to indicate that they had become semi-solidified/solidified characterized by certain/non displacement of the bubbles at the ends of the tubes.

Fatty acids composition

Table 3 outlines the fatty acids composition of the palm olein feed and hydrogenated oil-glycerol mixture (1:1 glycerol-to-oil molar ratio, 10 mm gap, 1 L min⁻¹ He flow rate, ambient temperature initially, 75 W plasma discharge power, 12 h reaction time). The feed contained 12 fatty acid types, comprising 40.56% saturated fatty acids with palmitic acid (C16:0) being predominant. The unsaturated fatty acids comprised 57.83%, with oleic acid (C18:1 n-9 *cis*) being the most prevalent at 42.98%, followed by linoleic acid (C18:2 n-6 *cis*) at 14.85%. The hydrogenated product showed 9 fatty acid types, with palmitic acid (C16:0) being the highest at 27.95%, followed by oleic acid (C18:1 n-9 *cis*) at 32.02%, linoleic acid (C18:2 n-6 *cis*) at 11.26%, and *trans*-fat detection of C18:1 n-9 *trans* at 10.01%.

When comparing the compositions, it is evident that palmitic acid (C16:0), oleic acid (C18:1 n-9 *cis*), linoleic acid (C18:2 n-6 *cis*), and α -linolenic acid (C18:3 n-3) decreased, while lauric acid (C12:0), myristic acid (C14:0), palmitoleic acid (C16:1), stearic acid (C18:0), and C18:1 n-9 *trans* increased. This shift indicates a reduction in mono-, di-, and tri-unsaturated fatty acids alongside an increase in saturated chains, being typical outcomes of hydrogenation affecting unsaturated carbon atoms. Remarkably, C12:0 and C14:0 also increased. Unlike C16:0 which substantially decreased, it is possibly due to the energetic energy of plasma radicals and reactive species provided by plasma that could break longer fatty acid chains into shorter ones. These findings align with the previous investigation by Yepez and Keener²⁵.

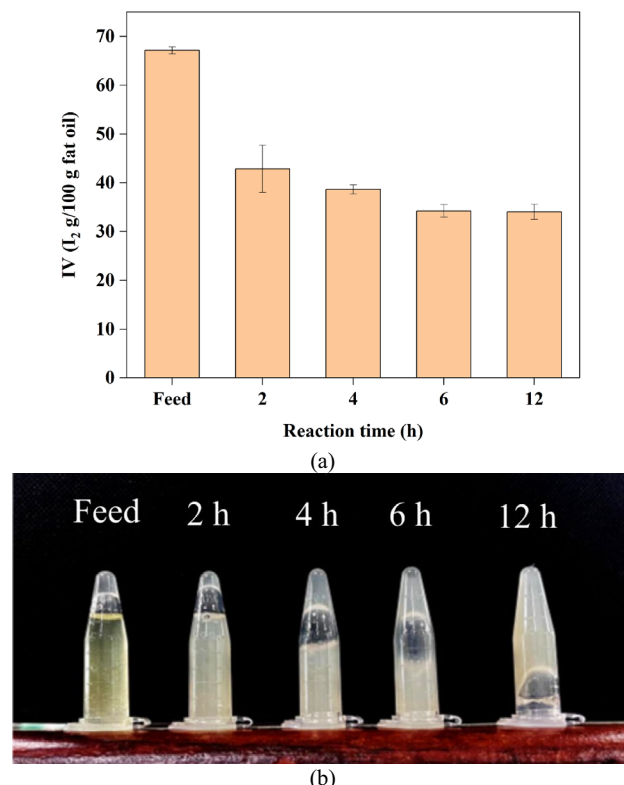


Figure 10. (a) IV of oil in the investigation of reaction time, and (b) pictures of samples (1:1 oil-to-glycerol molar ratio, 10 mm gap size, 1 L min⁻¹ He gas flow rate, 75 W plasma discharge power, and ambient temperature with initial temperature of 27 °C).

Fatty acid composition	Palm olein feed (%)	Hydrogenated palm olein-glycerol** (%)	Absolute difference (%)
C8:0	0.02	–	0.02
C10:0	0.02	–	0.02
C12:0	0.35	0.41 ↑	0.06
C14:0	0.96	1.38 ↑	0.42
C15:0	–	–	–
C16:0	33.92	27.95 ↓	5.97
C16:1	0.20	0.22 ↑	0.02
C17:0	–	–	–
C17:1	–	–	–
C18:0	4.92	6.00 ↑	1.08
C18:1 n-9 cis	42.67	38.02 ↓	4.65
C18:1 n-9 trans	–	10.01 ↑	10.01
C18:2 n-6 cis	14.64	11.26 ↓	3.38
C18:2 n-6 trans	–	–	–
C18:3 n-3	0.21	0.46 ↓	0.25
C20:0	0.37	–	0.37
C20:1 n-9	0.11	–	0.11
C24:0	–	–	–
SFA*	40.56	35.74	4.82
MUFA*	42.98	48.25	5.27
PUFA*	14.85	11.72	3.10
Unidentified	1.61	4.29	2.68

Table 3. Summary of fatty acid compositions. *SFA saturated fatty acid, MUFA monounsaturated fatty acid, PUFA polyunsaturated fatty acid. **1:1 glycerol-to-oil molar ratio, 10 mm gap, 1 L min⁻¹ He flow rate, ambient temperature initially, 75 W plasma discharge power, 12 h reaction time.

FTIR analysis

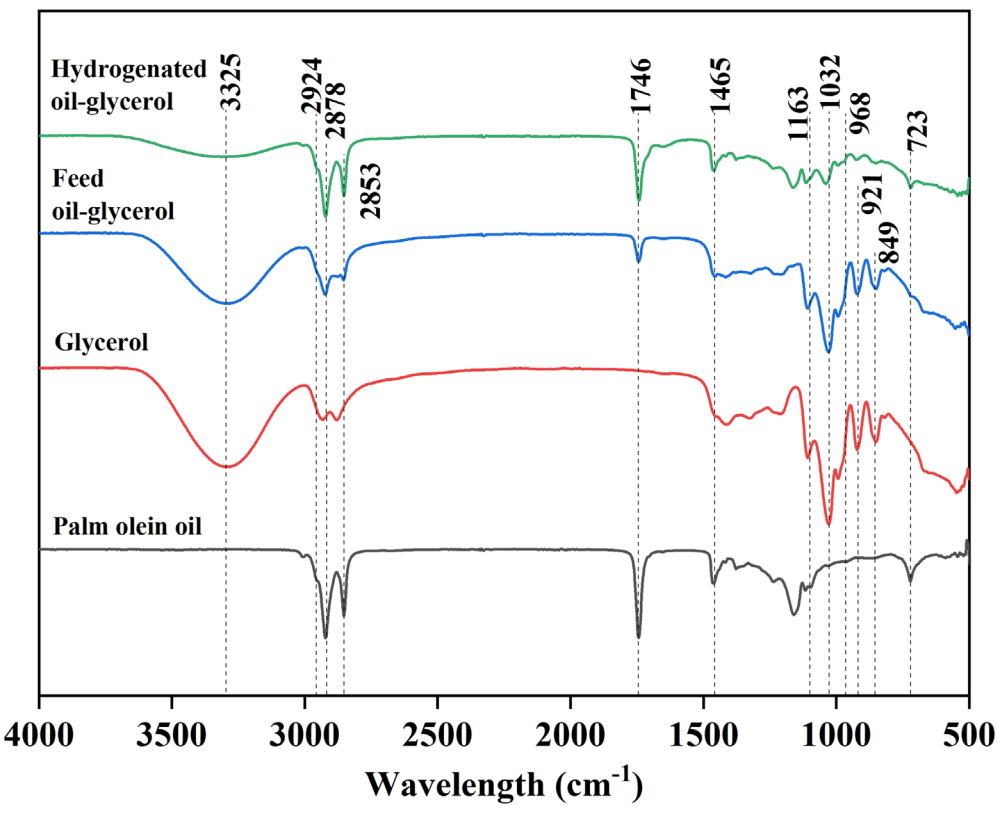
The functional groups of the oil-glycerol mixture before and after hydrogenation are presented in (Fig. 11a). The feed exhibited the characteristic peak at 3325 cm⁻¹ indicating O-H stretching of glycerol⁴⁶, and the two peaks at around 2924 and 2853 cm⁻¹ indicating C-H stretching originating from palm olein which is oleic and palmitic acid⁴⁶, and C-H stretching at 2878 cm⁻¹ originating from glycerol⁴⁷. The peak at 1746 cm⁻¹ indicated C=O stretching⁴⁶.

The hydrogenated oil-glycerol mixture after the reaction indicated a distinctly different peak at 3265 cm⁻¹ representing O-H stretching. The O-H group became much less intense because the H atoms were extracted becoming H radicals and cooperating with the C=C bonds of the oil. The decreasing peaks (Fig. 11b) at around 2878–2853 cm⁻¹ (C-H stretch from oleic and palmitic acids) could indicate a reduction of oleic acid and palmitic acid⁴⁸. The oleic acid appeared to be converted into saturated fatty acids by hydrogenation, while the palmitic acid might transform into shorter hydrocarbon chains by plasma scissoring. The decreased peak at 1746 cm⁻¹ (C=O group) could indicate changes in the FFA content from triglyceride fats⁴⁸, while the -HC=CH (*trans*-) group⁴⁹ in the hydrogenated oil initially appearing at 968 cm⁻¹ was still slightly observed as detected 10% *trans*-fat in GC analysis (Table 3).

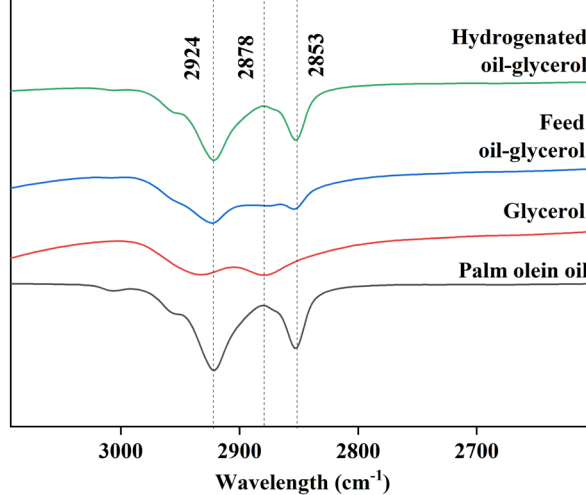
Notably, the peak at 1465 cm⁻¹ associated with C-H bending emerged⁵⁰, while the presence of the peak at 1163 cm⁻¹ indicated the stretching of the C-O ester group³⁷. The formation of this peak possibly stemmed from the disintegration of the hydrogen atom from C-OH in glycerol. Consequently, the intensity of the O-H peak at 921 cm⁻¹ and the C-O stretching peak at 1032 cm⁻¹ (Fig. 11c) appeared diminished³⁷.

Optimal plasma hydrogenation conditions to prevent *trans*-fat formation

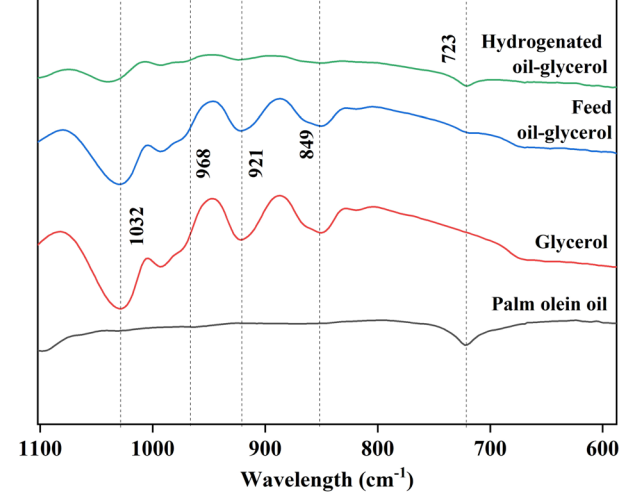
Previous investigations revealed that one of the factors determining the predicted formation of *trans*-fat in conventional hydrogenation is the deodorization process⁵¹. The process has a wider range of times and temperatures to remove pesticides and light polychromatic hydrocarbons from vegetable oil. In plasma hydrogenation, the temperature factor is also the cause of the *trans*-fat formation as shown in the FTIR determination at a wavelength of 968 cm⁻¹⁴⁹. This temperature factor is very dependent on the applied plasma discharge power, as it was revealed in the present study that the difference in plasma discharge power resulted in a difference in the reaction temperature. The initial temperature for all plasma power varieties was at room temperature, and the final temperature after 2 h rose to 40, 60, and 80 °C at 35, 50, and 75 W, respectively, of plasma discharge power (see Supplementary Data Fig. S1). A study by Puprasit et al.²⁰ observed that a temperature rise was attributed to the exothermic nature of the hydrogenation reaction, which supports the present investigation. Although prolonging the plasma exposure time to 12 h reduced the IV substantially and produced a desirable solid fat (Sect. “Influence of reaction time”), the GC-MS analysis revealed a remarkably high *trans*-fat composition (Table 3). The saturated fatty acids including C12:0, C14:0, and C18:0 increased, while the unsaturated fatty acids including C18:1 n-9



(a)



(b)



(c)

Figure 11. FTIR spectra of feed palm oil-glycerol and hydrogenated palm oil-glycerol. (a) Full spectra, (b) Zoom-in peak at $2924\text{--}2853\text{ cm}^{-1}$, (c) Zoom-in peak at $1032\text{--}723\text{ cm}^{-1}$.

cis, C18:2 n-6 *cis*, and C18:3 n-3 decreased. Notably, there was *trans* fatty acid formation of 10.01%. To reduce the amount of *trans*-fat, which was also the primary goal of the present investigation, another experiment was performed with a low plasma discharge power of 35 W, resulting in the mixed liquid temperature rise of only 40 °C. The other process parameters were a 1:1 molar ratio of glycerol to oil, 10 mm of gap size, 1 L min⁻¹ of He gas flow rate, and ambient temperature initially. The compared results are shown in (Fig. 12a).

The finding was that the IV reduction at 2, 4, 6, and 12 h at 35 W was 56.61 ± 3.23 , 50.61 ± 0.54 , 44.61 ± 2.76 , and 31.61 ± 1.11 , respectively. This finding is consistent with those reported by Liu and Lu⁵², which observed similar trends in the temperature effect to the *trans*-fat production using p-toluenesulfinic acid catalyst. It was explained that reaction temperature of 100 °C and above have been significantly result in 79.6% *trans*-fat

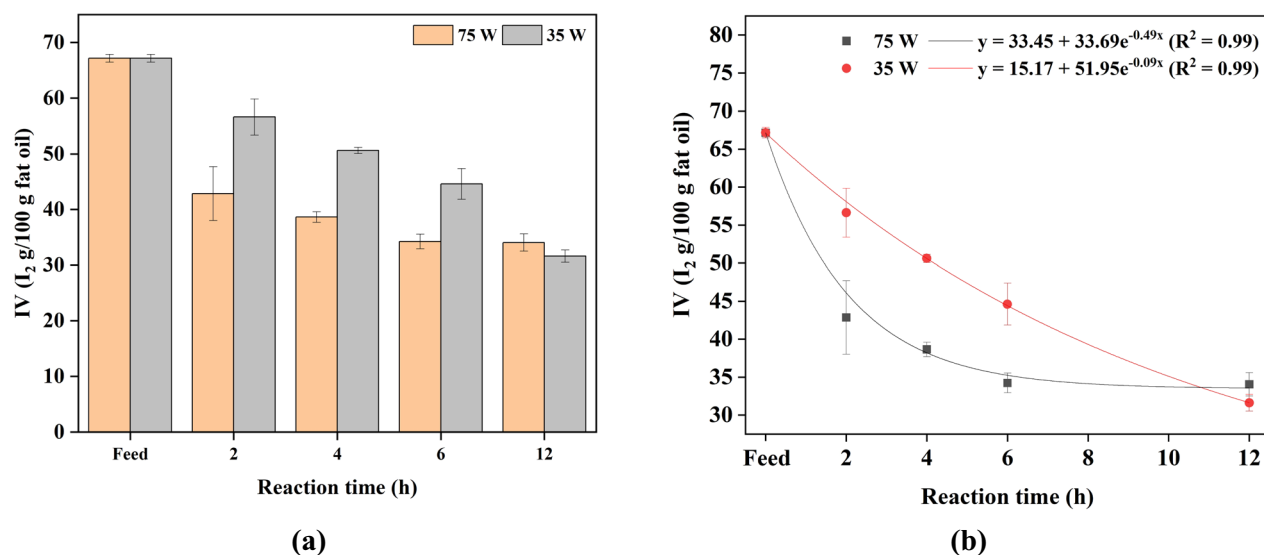


Figure 12. (a) Comparative IV result after plasma discharge power adjustment from 75 to 35 W, and (b) hydrogenation rate analysis from the exponential model.

production. It was stated that *cis-trans* isomerization caused by free radical intermediates from the catalyst has a definite temperature. This consistency across different studies reinforces the understanding that high temperature catalyzes the formation of *trans* fats, highlighting the need for controlled hydrogenation conditions to minimize *trans*-fat production. In terms of the plasma process, it offered the released heat at the electrodes. To reduce the *trans*-fatty acid and accelerate the reaction rate, several factors need to be considered, including the discharge power to provide the lowest operational temperature, the stirring rate to allow the most suitable mass transfer, the modified DBD power supply to decrease self-heating.

Figure 12b illustrates that the reduction in IV occurred more rapidly at 75 W compared to 35 W. Specifically, by following the exponential fitting model fitted by OriginLab software, the rate of IV reduction for each case was proposed. According to the model, the hydrogenation rate can be calculated from the first derivative of the exponential plot. The rate of IV reduction along the time via hydrogenation rate for the 75 W case was $-16.508e^{-0.49x}$, while the rate for the 35 W case was $-4.67e^{-0.09x}$. The R^2 -value obtained from both cases was 0.99, indicating that both cases have a 0.99 variation in the dependent variable (IV) that is statistically predicted by the exponential model as similar to the rate of reactant concentration disappearing along the reaction time ($-dC_A/dt$). Although it was found that the 35 W condition exhibited a slower IV reduction, the 12 h reaction time still gave the same IV result with zero quantities of *trans* fat as shown in (Table 4).

Table 4 presents the fatty acid compositions of palm olein feed, 75-W hydrogenated oil-glycerol, and 35-W hydrogenated oil-glycerol maintaining other fixed parameters of 1:1 molar ratio of glycerol to oil, 10 mm gap size, 1 L min⁻¹ He flow rate, and ambient temperature initially. The 35-W case contained 8 fatty acid types, comprising 58.61% saturated fatty acids, predominantly palmitic acid (C16:0) at 44.51%. The unsaturated fatty acids comprised 39%, with oleic acid (C18:1 n-9 *cis*) being the most prevalent at 35.24%, followed by linoleic acid (C18:2 n-6 *cis*) at 3.86%. The 35-W case exhibited a polyunsaturated fatty acid content reduction of 10.99% and a total monounsaturated fatty acid content decrease of 7.74%. This suggests that the hydrogenation of mono- and polyunsaturated fatty acids involves the cleavage of the double bond by the provision of a hydrogen atom from glycerol. An absence of elaidic acid (C18:1 n-9 *trans*) was observed (0%). In comparison with margarine production conducted by Puprasit et al.¹⁹ with a small amount of *trans*-fat present (1.44%), the present work can be a novel reference and competitive method as it does not involve the use of hydrogen gas.

Table 4 indicates a small difference in the total fatty acid composition of the two cases. The total fatty acid percentage of the 75-W case was 95.71% while it was 97.71% for the 35-W case. The mass of the feed oil-glycerol before and after the reaction was also investigated and is presented in (Table 5). For the 75-W case, the liquid mixture lost around 0.78 g, whereas the 35-W case lost around 0.31 g after plasma hydrogenation. For the change in fatty acids composition, C16:0 was notably increased, while there was a small number of C16:1 and without unsaturated sixteen carbon chain presence in feed. This is because the bond-cracking process of oil molecules could occur in the plasma process^{53,54}. The C16:0 was generated by the bond breaking of C18:0 at the ethyl group ($C_2H_5-nC_1H_{2i+1}$), which is the weakest bond in alkene (bold letter stands for the cracking group)⁵⁵. The process of becoming C16:0 released the small products, including ethyl and methyl radicals, in the gas phase and moving out of the reaction chamber with the plasma gas. This is related to the mass loss that took place in this study. Higher mass loss was observed when using a higher power of 75 W. The higher applied plasma power offered stronger plasma filaments with higher energy of generated reactive species, resulting in a higher chance of bond breaking. Also, the direct contact of the strong filaments with the mixed solution might cause some palm oil to mix in the glycerol layer. Therefore, the amount of oil changed after the separation process.

Fatty acid composition	Palm olein feed (%)	Hydrogenated palm olein-glycerol by 75 W DBD plasma for 12 h (%)	Hydrogenated palm olein-glycerol by 35 W DBD plasma for 12 h (%)	Hydrogenated palm olein by 21.85 W DBD plasma for 12 h (%)
		(Present work)		(Previous work) ¹⁹
C8:0	0.02	–	–	–
C10:0	0.02	–	–	–
C12:0	0.35	0.41	0.42	–
C14:0	0.96	1.38	1.25	0.89
C15:0	–	–	–	0.03
C16:0	33.92	27.95	44.51	39.47
C16:1	0.20	0.22	–	0.13
C17:0	–	–	–	0.05
C17:1	–	–	–	–
C18:0	4.92	6	10.27	5.51
C18:1 n-9 <i>cis</i>	42.67	38.02	35.24	43.39
C18:1 n-9 <i>trans</i>	–	10.01	–	1.44
C18:2 n-6 <i>cis</i>	14.64	11.26	3.86	8.19
C18:2 n-6 <i>trans</i>	–	–	–	–
C18:3 n-3	0.21	0.46	–	0.10
C20:0	0.37	–	0.44	–
C20:1 n-9	0.11	–	–	–
C24:0	–	–	1.72	–
SFA*	40.56	35.74	58.61	45.95
MUFA*	42.98	48.25	35.24	44.96
PUFA*	14.85	11.72	3.86	8.29
Total FA*	98.39	95.71	97.71	99.20

Table 4. Summary of fatty acid compositions. *SFA saturated fatty acid, MUFA monounsaturated fatty acid, PUFA polyunsaturated fatty acid, FA fatty acid. Significant values are in bold.

Condition	Total mass of oil-glycerol (g)	Total fatty acids (%)
Feed oil-glycerol	32.06	98.39
After 75 W plasma	31.28	95.71
After 35 W plasma	31.75	97.71

Table 5. Summary of mass balance.

The thermal image processing of the DBD plasma and the oil-glycerol mixture is presented in (Fig. 13a–d). It was found that the highest temperature in one spot of the plasma streamer was about 225° C (Fig. 13d). This observation suggests that localized regions within the plasma streamer could cause the mass change in palm oil. With heat, oil degradation may also produce gel/solid residues⁵⁶. These residues can accumulate on the equipment surfaces and lead to an imbalance between the mass of the exiting feed material and that of the material entering the reaction chamber⁵⁷. Another contributing factor for mass loss could be degradation or chemical modification during sample preparation or analysis⁵⁸, leading to the formation of compounds not detected by the GC-MS as fatty acids or that cannot be quantified accurately.

Formation of plasma reactive species during reaction

The reactive species generated during the reaction were detected using optical emission spectroscopy (OES) in the range of 200–1100 nm, as illustrated in (Fig. 14). When the plasma was on, the energetic electrons forming in the plasma could collide with gas molecules to create more He species, as there were eight detected peaks corresponding to He plasma at 356, 492, 501, 587, 668, 706, 778, and 846 nm⁵⁹. Hydrogen species with the highest intensity in the range of Balmer and Paschen regions, named H^(A, B, C, D, and E) were also observed²⁵. This implies that the plasma successfully attacked the bonded hydrogen atoms in the molecules of glycerol becoming free hydrogen species in the system.

Physical characteristics of optimal hydrogenated oil-glycerol mixture: AV, SMP, and texture

The AV, SMP, spreadability, and hardness values of the synthesized product based on the 1:1 molar ratio oil to glycerol, 1 L min⁻¹ H₂ flow rate, 35 W plasma discharge power, 12 h reaction time, and ambient initial reaction temperature are shown in (Table 6).

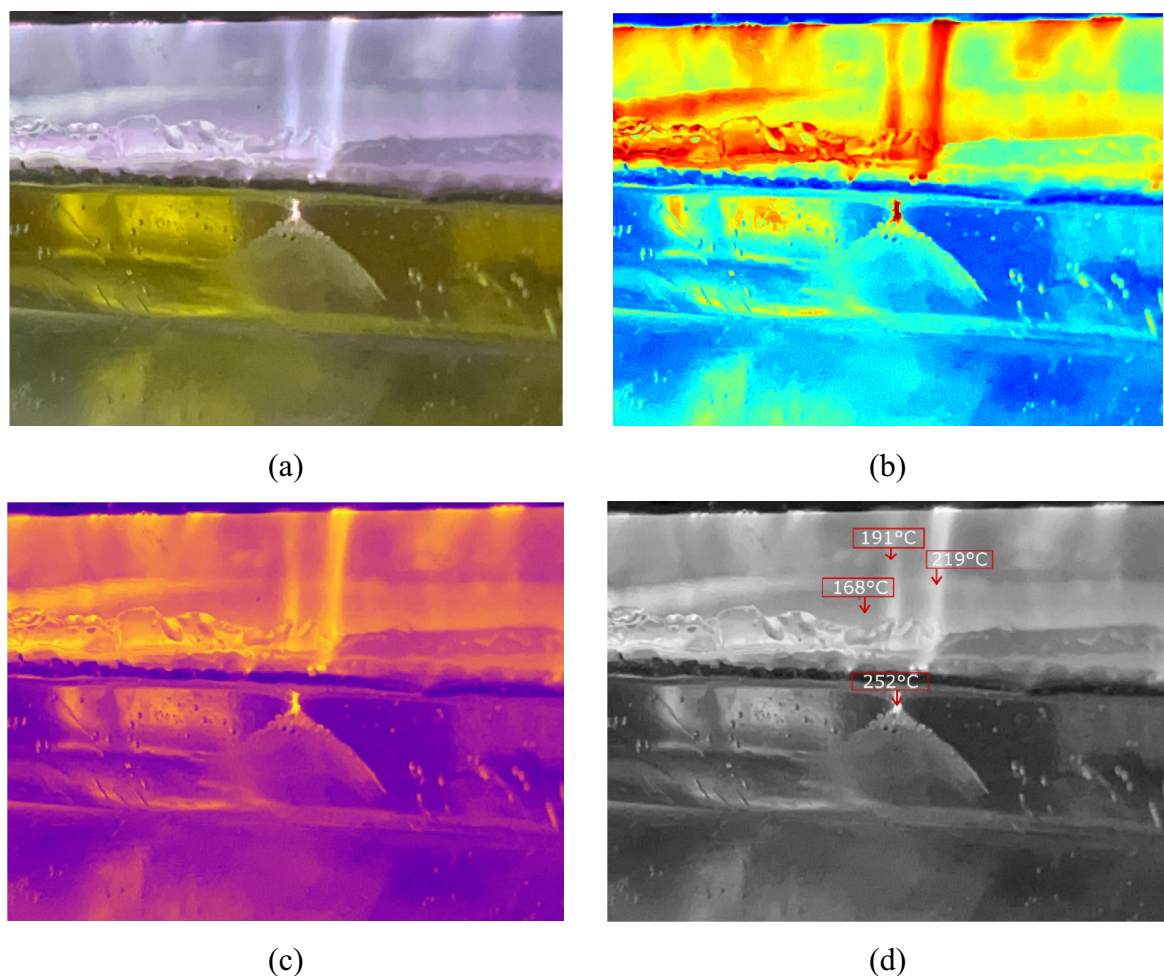


Figure 13. Observed plasma hotspot during experiment via thermal image processing: (a) RGB visible-light image of feed oil-glycerol, (b) Jet-thermal colormaps, (c) Plasma-thermal colormaps, and (d) Gray-thermal colormaps with temperature.

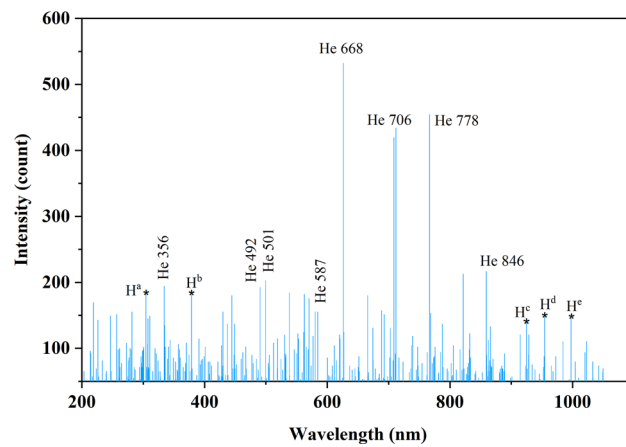


Figure 14. Optical emission spectrum of He plasma during hydrogenation.

The AV serves as a fundamental indicator of product quality, reflecting the acid content in fats or oils because of hydrolytic deterioration, commonly known as rancidity, of the triacylglycerol. The results indicate a slight increase in AV from 0.47 to 0.51, an 8.51% gain. It was within the acceptable range, which should not exceed 0.6 mg KOH/g fats⁶⁰. This increase can be attributed to the presence of hydrogen radicals from glycerol, which possess sufficient energy to catalyze the hydrolysis of triglycerides into free fatty acids and glycerol, particularly

Sample	AV (mg KOH/g)	SMP (°C)	Spreadability (Nm)	Hardness (N)
Feed	0.47±0.01	32*	–	–
Product (this work)	0.51±0.05	35.7±1.3	0.027±0.001	8.71±0.56
Commercial product (lotus brand)	0.50±0.67	33.2±0.5	0.025±0.008	8.00±0.24

Table 6. Characterization of synthesized product from optimal process parameters (1:1 molar ratio oil to glycerol, 1 L min⁻¹ H₂ flow rate, 35 W plasma discharge power, 12 h reaction time, and ambient initial reaction temperature). *Data obtained from Wongjaikham et al.²¹.

during the hydrogenation process. Consequently, this hydrolysis leads to an elevation in the concentration of free fatty acids, thus contributing to the observed increase in AV.

The SMPs of the feed and product were recorded as 32 and 35.7 °C, respectively. A longer hydrogenation duration resulted in a higher SMP as the oil became more hardened due to a greater content of saturated fatty acids, agreeing with the decreasing IV²¹. The product exhibited a stable texture at room temperature. This stability is useful for prolonging the storage shelf-life. Supporting the agreement from Rajah et al.²¹, the investigation showed the range of melting point of hydrogenated palm oil of 32–37 °C. For the SMPs of margarine, the reported SMP for bakery & pastry products was 31.2–34.9 °C in Turkey⁶¹, and 32–41.31 °C in Iran⁶². Therefore, the produced product exhibiting the SMP of 35.7 °C was within the usable range for bakery purposes.

Spreadability is primarily recognized as the primary textural characteristics of margarine, which significantly impact consumer acceptance and render it acceptable for various applications. The spreadability of margarine can be predicted by the quantification of hardness value. It is quantified by the maximum force attained upon initial compression. The margarine with enhanced hardness exhibited less spreadability⁶³. The spreadability and hardness values were recorded as 0.027±0.001 Nm and 8.71±0.56 N, respectively.

Comparison margarine production over plasma treatment

In this section, comparative studies on fatty acids conversion by plasma hydrogenation methods is described. The summarized results based on the basic product properties and several parameters are shown in (Table 7).

Material & process	Product property	Energy consumption (MJ/kg)	Time consumption (h)	Production cost (USD/L)	Ref
Palm olein oil + glycerol via DBD plasma	Iodine value: 31.61 g I ₂ /100 g fat	46.8	12	3.29	This work
	Acid value: 0.51 mg KOH/g fats				
	Slip melting point: 35.7 °C				
	Spreadability: 0.027 Nm				
	Hardness: 8.71 N				
	Trans-fat: 0%				
Palm oil via catalyst-free microwave plasma	Iodine value: 32.51 g I ₂ /100 g fat	48	3–4	N/A	21
	Acid value: 0.17 mg KOH/g fats				
	Slip melting point: 36.7 °C				
	Spreadability: 4.5±0.65 N.s				
	Hardness: 0.8 N				
	Trans-fat: 4.23%				
Palm & Soybean oil via DBD plasma	Iodine value: 48.39 g I ₂ /100 g fat	69.92	4	2.99	19,64
	Acid value: 43% reduction				
	Slip melting point: 28 °C				
	Spreadability: N/A				
	Hardness: 8.5 N				
	Trans-fat: 1.44%				
Soybean oil via high-voltage atmospheric cold plasma (HVACP)	Iodine value: 92 g I ₂ /100 g fat	960	12	N/A	25
	Acid value: N/A				
	Slip melting point: N/A				
	Spreadability: N/A				
	Hardness: N/A				
	Trans-fat: 0%				
Vegetable oils via high temperature and high-pressure method with catalyst	N/A	4	N/A	N/A	65

Table 7. Recent investigations of compared method for margarine production. *N.A. means not available/no data provided.

There are scarce sources of scientific papers available that converting fatty acids by cold plasma hydrogenation methods, despite of the use of glycerol includes in research studies. Therefore, the comparison between the plasma hydrogenation with glycerol and the conventional plasma hydrogenation (with H₂ gas) methods was only done based on four parameters: product properties, energy consumption, time consumption, and cost production.

Based on Wongjaikham et al.'s microwave plasma approach²¹, the energy consumption was found higher as compared to this study with 4.23% *trans*-fat product, while Puprasit et al.^{19,64} proposed 1.44% *trans*-fat product with a slightly competitive energy consumption of 0.437 kWh. Although Yepez & Keener²⁵ found a successful zero *trans*-fat product with the pioneering research on this process, the energy consumption was also higher compared to this study. The summarized results showed that this frontier novel method for fatty acids conversion has significant product properties that have not been previously discovered. However, additional research is required to explore the pathway mechanism and optimization parameters to enhance energy efficiency while maintaining cost-effective production.

Conclusions

The parallel-plate DBD plasma system to produce *trans*-fat-free margarine using edible palm olein as the feed and glycerol as the principal source of hydrogen was successfully developed. The most suitable process parameters were: 1:1 molar ratio of oil to glycerol, 10 mm gap size, 1 L min⁻¹ of He flow rate, 35 W of plasma discharge power, and ambient initial temperature for 12 h of reaction time. No *trans*-fat was detected by GC-MS in the synthesized product. The IV decreased from 67.16 ± 0.70 to 31.61 ± 1.1. The product exhibited a solid texture with spreadability and hardness values of 0.027 ± 0.001 Nm and 8.71 ± 0.56 N, respectively. The measured SMP of 35.7 °C was within the usable range for bakery purposes. The AV was 0.51 mg KOH/g, being within the acceptable range of 0.6 mg KOH/g. The investigation showcases the effective utilization of non-thermal DBD plasma for the hydrogenation of palm olein, exhibiting a favorable absence of hydrogen gas and a catalyst showing no production of *trans*-fatty acids. The approach presents a potential opportunity to provide a viable option for effective margarine production in the food and oils industry.

Data availability

The datasets used and/or analysed during the current study are available from the corresponding author on reasonable request.

Received: 1 May 2024; Accepted: 26 July 2024

Published online: 09 August 2024

References

- Chilakamary, C. R., Sakinah, A. M. M., Zularisam, A. W. & Pandey, A. Glycerol waste to value added products and its potential applications. *Syst. Microbiol. Biomanuf.* **1**, 378–396. <https://doi.org/10.1007/s43393-021-00036-w> (2021).
- Rozulan, N., Halim, S. A., Razali, N. & Lam, S. S. A review on direct carboxylation of glycerol waste to glycerol carbonate and its applications. *Biomass Conv. Bioref.* **12**, 4665–4682. <https://doi.org/10.1007/s13399-022-02540-y> (2022).
- Editors, B. Glycerol definition, <<https://biologydictionary.net/glycerol/#cosmetics-and-food>> (2017).
- Gu, Y., Barrault, J. & Jérôme, F. Glycerol as an efficient promoting medium for organic reactions. *Adv. Synth. Catal.* **350**, 2007–2012. <https://doi.org/10.1002/adsc.200800328> (2008).
- Naik, M. K., Naik, S. N. & Mohanty, S. Enzymatic glycerolysis for conversion of sunflower oil to food based emulsifiers. *Catal. Today* **237**, 145–149. <https://doi.org/10.1016/j.cattod.2013.11.005> (2014).
- Tamošiūnas, A., Gimžauskaitė, D., Uscila, R. & Aikas, M. Thermal arc plasma gasification of waste glycerol to syngas. *Appl. Energy* **251**, 113306. <https://doi.org/10.1016/j.apenergy.2019.113306> (2019).
- Kumar, L. R., Yellapu, S. K., Tyagi, R. D. & Drogui, P. Purified crude glycerol by acid treatment allows to improve lipid productivity by yarrowia lipolytica SKY7. *Process Biochem.* **96**, 165–173. <https://doi.org/10.1016/j.procbio.2020.06.010> (2020).
- Chilakamary, C. R. *et al.* Bioconversion of glycerol into biofuels—Opportunities and challenges. *Bioenerg. Res.* **15**, 46–61. <https://doi.org/10.1007/s12155-021-10353-6> (2022).
- WHO. REPLACE *trans* fat: An action package to eliminate industrially produced trans-fatty acids. <<https://www.who.int/publications/item/9789240021105>> (2021).
- Ghebreyesus, T. A. & Frieden, T. R. REPLACE: A roadmap to make the world *trans* fat free by 2023. *Lancet* **391**, 1978–1980. [https://doi.org/10.1016/S0140-6736\(18\)31083-3](https://doi.org/10.1016/S0140-6736(18)31083-3) (2018).
- Brát, J. & Pokorný, J. Fatty acid composition of margarines and cooking fats available on the czech market. *J. Food Compos. Anal.* **13**, 337–343. <https://doi.org/10.1006/jfca.1999.0877> (2000).
- Longhi, R. Dietary interventions in liver disease. In *Trans Fatty Acid in the Liver and Central Nervous System* (ed. Longhi, R.) (Elsevier, 2019).
- Ginter, E. & Simko, V. New data on harmful effects of *trans*-fatty acids. *Bratisl. Lek. Listy* **117**, 251–253. https://doi.org/10.4149/bll_2016_048 (2016).
- Stender, S., Astrup, A. & Dyerberg, J. Ruminant and industrially produced trans fatty acids: Health aspects. *Food Nutr. Res.* <https://doi.org/10.3402/fnr.v52i0.1651> (2008).
- Ferlay, A., Bernard, L., Meynadier, A. & Malpuech-Brugere, C. Production of trans and conjugated fatty acids in dairy ruminants and their putative effects on human health: A review. *Biochimie* **141**, 107–120. <https://doi.org/10.1016/j.biochi.2017.08.006> (2017).
- Niforou, A. *et al.* On account of trans fatty acids and cardiovascular disease risk—There is still need to upgrade the knowledge and educate consumers. *Nutr. Metab. Cardiovasc. Dis.* **32**, 1811–1818. <https://doi.org/10.1016/j.numecd.2022.05.010> (2022).
- Kiralan, M., Ketenoglu, O. & Kiralan, S. S. in *Bioactive Natural Products Studies in Natural Products Chemistry* 313–343 (2021).
- Thirumdas, R. Partial hydrogenation of oils using cold plasma technology and its effect on lipid oxidation. *J. Food Sci. Technol.* **60**, 1674–1680. <https://doi.org/10.1007/s13197-022-05434-z> (2023).
- Puprasit, K. *et al.* Non-thermal dielectric barrier discharge plasma hydrogenation for production of margarine with low trans-fatty acid formation. *Innov. Food Sci. Emerg. Technol.* <https://doi.org/10.1016/j.ifset.2020.102511> (2020).
- Puprasit, K. *et al.* Improved hydrogenation process for margarine production with no trans fatty acid formation by non-thermal plasma with needle-in-tube configuration. *J. Food Eng.* <https://doi.org/10.1016/j.jfoodeng.2022.111167> (2022).
- Wongjaikham, W. *et al.* Production of low *trans*-fat margarine by partial hydrogenation of palm oil using nature-friendly and catalyst-free microwave plasma technique. *Innov. Food Sci. Emerg. Technol.* <https://doi.org/10.1016/j.ifset.2022.103107> (2022).

22. Tamošiūnas, A. *et al.* Waste glycerol gasification to syngas in pure DC water vapor arc plasma. *Int. J. Hydrot. Energy* **47**, 12219–12230. <https://doi.org/10.1016/j.ijhydene.2021.06.203> (2022).
23. Zou, X. *et al.* Plasma activated oil: Fast production, reactivity, stability, and wound healing application. *ACS Biomater. Sci. Eng.* **5**, 1611–1622. <https://doi.org/10.1021/acsbiomaterials.9b00125> (2019).
24. Long, Y. D. & Fang, Z. Hydrothermal conversion of glycerol to chemicals and hydrogen: Review and perspective. *Biofuels Bioprod. Bioref.* **6**, 686–702. <https://doi.org/10.1002/bbb.1345> (2012).
25. Yepez, X. V. & Keener, K. M. High-voltage atmospheric cold plasma (HVACP) hydrogenation of soybean oil without *trans*-fatty acids. *Innov. Food Sci. Emerg. Technol.* **38**, 169–174. <https://doi.org/10.1016/j.ifset.2016.09.001> (2016).
26. Wolfson, A., Dlugy, C., Shotland, Y. & Tavor, D. Glycerol as solvent and hydrogen donor in transfer hydrogenation–dehydrogenation reactions. *Tetrahedron Lett.* **50**, 5951–5953. <https://doi.org/10.1016/j.tetlet.2009.08.035> (2009).
27. Chizoba Ekezie, F. G., Sun, D. W. & Cheng, J. H. A review on recent advances in cold plasma technology for the food industry: Current applications and future trends. *Trends Food Sci. Technol.* **69**, 46–58. <https://doi.org/10.1016/j.tifs.2017.08.007> (2017).
28. Kim, J. H. & Min, S. C. Moisture vaporization-combined helium dielectric barrier discharge-cold plasma treatment for microbial decontamination of onion flakes. *Food Control* **84**, 321–329. <https://doi.org/10.1016/j.foodcont.2017.08.018> (2018).
29. Toyokawa, Y. *et al.* Roller conveyer system for the reduction of pesticides using non-thermal gas plasma—A potential food safety control measure?. *Food Control* **87**, 211–217. <https://doi.org/10.1016/j.foodcont.2017.12.030> (2018).
30. Laroque, D. A. *et al.* Cold plasma in food processing: Design, mechanisms, and application. *J. Food Eng.* <https://doi.org/10.1016/j.jfoodeng.2021.110748> (2022).
31. Grunberg, L. & Nissan, A. H. Mixture law for viscosity. *Nature* **164**, 799–800. <https://doi.org/10.1038/164799b0> (1949).
32. Graham, T. XXVIII. On the motion of gases. *Phil. Trans. R. Soc. Lond.* **136**, 573–631. <https://doi.org/10.1098/rstl.1846.0029> (1846).
33. Amorim, T. L. *et al.* Prediction of fatty acids in chocolates with an emphasis on C18:1 *trans* fatty acid positional isomers using ATR-FTIR associated with multivariate calibration. *J. Agric. Food Chem.* **68**, 10893–10901. <https://doi.org/10.1021/acs.jafc.0c04316> (2020).
34. Schwartz, S. & Warneck, P. Units for use in atmospheric chemistry (IUPAC recommendations 1995). *Pure Appl. Chem.* **67**, 1377–1406. <https://doi.org/10.1351/pac199567081377> (1995).
35. Tube, G. *Palm Oil Properties-Temperature Viscosity Heat Capacity*, <<https://tubingchina.com/Palm-Oil-Properties-Temperature-Viscosity-Heat-Capacity-Conductivity-Density-Viscosity.htm>>.
36. Sheely, M. L. Glycerol viscosity tables. *Ind. Eng. Chem.* **24**, 1060–1064. <https://doi.org/10.1021/ie50273a022> (1932).
37. Kongprawes, G. *et al.* Dielectric barrier discharge plasma for catalytic-free palm oil hydrogenation using glycerol as hydrogen donor for further production of hydrogenated fatty acid methyl ester (H-FAME). *J. Clean. Prod.* <https://doi.org/10.1016/j.jclepro.2023.136724> (2023).
38. Al-Moameri, H., Jaf, L. & Suppes, G. J. Viscosity-dependent frequency factor for modeling polymerization kinetics. *Rsc. Adv.* **7**, 26583–26592. <https://doi.org/10.1039/c7ra01242j> (2017).
39. Zhang, Y., Zheng, J., Qu, X. & Chen, H. Design of a novel non-equilibrium plasma-based water treatment reactor. *Chemosphere* **70**, 1518–1524. <https://doi.org/10.1016/j.chemosphere.2007.09.013> (2008).
40. Yoon, S.-Y. *et al.* Mutual interaction between plasma characteristics and liquid properties in AC-driven Pin-to-liquid discharge. *Sci. Rep.* **8**, 12037. <https://doi.org/10.1038/s41598-018-30540-4> (2018).
41. Ohtsu, Y. & Fujita, H. Influences of gap distance on plasma characteristics in narrow gap capacitively coupled radio-frequency discharge. *Jpn. J. Appl. Phys.* **43**, 795. <https://doi.org/10.1143/JJAP43.795> (2004).
42. Harris, J., Phan, A. N. & Zhang, K. Cold plasma catalysis as a novel approach for valorisation of untreated waste glycerol. *Green Chem.* **20**, 2578–2587. <https://doi.org/10.1039/C8GC01163J> (2018).
43. Zhang, K. *et al.* A study on CO₂ decomposition to CO and O₂ by the combination of catalysis and dielectric-barrier discharges at low temperatures and ambient pressure. *Ind. Eng. Chem. Res.* **56**, 3204–3216. <https://doi.org/10.1021/acs.iecr.6b04570> (2017).
44. Şahin, N. & Tanışlı, M. Electron temperature estimation of helium plasma via line intensity ratio at atmospheric pressure. *Eur. Phys. J. Plus* <https://doi.org/10.1140/epjp/s13360-020-00685-1> (2020).
45. Bond Dissociation Energy, <<https://chem.libretexts.org/ga/page/30372>> (2022).
46. Sittinun, A. *et al.* Utilization of palm olein-based polyol for polyurethane foam sponge synthesis: Potential as a sorbent material. *J. Polym. Environ.* **28**, 3181–3191. <https://doi.org/10.1007/s10924-020-01834-4> (2020).
47. Danish, M., Mumtaz, M., Fakhar, M. & Rashid, T. D. U. Response surface methodology: An imperative tool for the optimized purification of the residual glycerol from biodiesel production process. *Chiang Mai J. Sci.* **44**, 1570–1582 (2016).
48. Che Man, Y. B., Moh, M. H. & van de Voort, F. R. Determination of free fatty acids in crude palm oil and refined-bleached-deodorized palm olein using fourier transform infrared spectroscopy. *J. Am. Oil Chem. Soc.* **76**, 485–490. <https://doi.org/10.1007/s11746-999-0029-z> (1999).
49. Li, Q. *et al.* Application of fourier transform infrared spectroscopy for the quality and safety analysis of fats and oils: A review. *Crit. Rev. Food Sci. Nutr.* **59**, 3597–3611. <https://doi.org/10.1080/10408398.2018.1500441> (2019).
50. Hashim, Z., Zaki, S. & Muhamad, I. Quality assessment of fried palm oils using fourier transform infrared spectroscopy and multivariate approach. *Chem. Eng. Trans.* **56**, 829–834. <https://doi.org/10.3303/CET1756139> (2017).
51. van Duijn, G., Dumelin, E. E. & Trautwein, E. A. *Improving the Fat Content of Foods* (Woodhead Publishing, 2006).
52. Liu, W. & Lu, G. H. *Cis-trans* isomerization of unsaturated fatty acids in edible oils to prepare *trans* fat. *Grasas y Aceites* <https://doi.org/10.3989/gya.0225181> (2018).
53. Kongprawes, G. *et al.* Low-temperature and atmospheric pressure plasma for palm biodiesel hydrogenation. *Sci. Rep.* **11**, 14224. <https://doi.org/10.1038/s41598-021-92714-x> (2021).
54. Hao, H., Lian, P., Gong, J. & Gao, R. Theoretical study on the hydrogenation mechanisms of model compounds of heavy oil in a plasma-driven catalytic system. *Catalysts* **8**, 381 (2018).
55. Wu, J., Ning, H., Ma, L. & Ren, W. Accurate prediction of bond dissociation energies of large n-alkanes using ONIOM-CCSD(T)/CBS methods. *Chem. Phys. Lett.* **699**, 139–145. <https://doi.org/10.1016/j.cplett.2018.03.041> (2018).
56. Kheirollahivash, M., Rashidi, F. & Moshrefi, M. M. Hydrogen production from methane decomposition using a mobile and elongating arc plasma reactor. *Plasma Chem. Plasma Process.* **39**, 445–459. <https://doi.org/10.1007/s11090-018-9950-y> (2019).
57. Matseh, I. *et al.* Comparison of mass balance and oil quality in plant refinery I and IV. *IOP Conf. Ser. Mater. Sci. Eng.* **801**, 012043. <https://doi.org/10.1088/1757-899X/801/1/012043> (2020).
58. Liu, K., Liu, Y. & Chen, F. Effect of storage temperature on lipid oxidation and changes in nutrient contents in peanuts. *Food Sci. Nutr.* **7**, 2280–2290. <https://doi.org/10.1002/fsn3.1069> (2019).
59. Samanta, K. K. *et al.* Effect of plasma treatment on physico-chemical properties of cotton. *Int. J. Eng. Res.* **3**, 2467 (2014).
60. Zaeroomali, M., Maghsoudlou, Y. & Aryaei, P. Effect of storage time on table margarine characterization in refrigerated temperature. *Eur. J. Exp. Biol.* **4**, 182–184 (2014).
61. Karabulut, I. & Turan, S. Some properties of margarines and shortenings marketed in Turkey. *J. Food Compos. Anal.* **19**, 55–58. <https://doi.org/10.1016/j.jfca.2004.06.016> (2006).
62. Esmaeili Fard, N., Bahmaei, M. & Eshratabadi, P. Comparison of physicochemical characteristics of margarine and butter in Iranian market during storage. *J. Pharm. Health Sci.* **4**, 181–191 (2016).

63. Fallahasgari, M., Barzegar, F., Abolghasem, D. & Nayebzadeh, K. An overview focusing on modification of margarine rheological and textural properties for improving physical quality. *Eur. Food Res. Technol.* **249**, 2227–2240. <https://doi.org/10.1007/s00217-023-04282-1> (2023).
64. Puprasit, K. *Production of low trans-fatty acid margarine by Plasma Hydrogenation* Doctoral thesis, Chulalongkorn University Theses and Dissertations (Chula ETD), 67–68. <https://doi.org/10.58837/CHULA.THE.2021.277> (2021).
65. Ladha-Sabur, A., Bakalis, S., Fryer, P. J. & Lopez-Quiroga, E. Mapping energy consumption in food manufacturing. *Trends Food Sci. Technol.* **86**, 270–280. <https://doi.org/10.1016/j.tifs.2019.02.034> (2019).

Acknowledgements

This research project is supported by the Second Century Fund (C2F), Chulalongkorn University. D. Wong-sawaeng, K. Ngaooswan, W. Kiatkittipong, and S. Assabumrungrat would also like to acknowledge support from the NSRF via the Program Management Unit from Human Resources and Institutional Development, Research and Innovation (Grant Number B05F640085).

Author contributions

I.P.: Investigation, Writing- original draft, Writing—review & editing. D.W.: Conceptualization, Methodology, Resources, Investigation, Writing- original draft, Writing—review & editing, Funding acquisition. G.K.: Writing—review & editing. K.N.: Writing—review & editing. W.K.: Writing—review & editing. P.H.: Supervision. P.S.: Writing—review & editing. S.A.: Supervision, Writing—review & editing. All authors reviewed the manuscript.

Competing interests

The authors declare no competing interests.

Additional information

Supplementary Information The online version contains supplementary material available at <https://doi.org/10.1038/s41598-024-68729-5>.

Correspondence and requests for materials should be addressed to D.W.

Reprints and permissions information is available at www.nature.com/reprints.

Publisher's note Springer Nature remains neutral with regard to jurisdictional claims in published maps and institutional affiliations.

Open Access This article is licensed under a Creative Commons Attribution-NonCommercial-NoDerivatives 4.0 International License, which permits any non-commercial use, sharing, distribution and reproduction in any medium or format, as long as you give appropriate credit to the original author(s) and the source, provide a link to the Creative Commons licence, and indicate if you modified the licensed material. You do not have permission under this licence to share adapted material derived from this article or parts of it. The images or other third party material in this article are included in the article's Creative Commons licence, unless indicated otherwise in a credit line to the material. If material is not included in the article's Creative Commons licence and your intended use is not permitted by statutory regulation or exceeds the permitted use, you will need to obtain permission directly from the copyright holder. To view a copy of this licence, visit <http://creativecommons.org/licenses/by-nc-nd/4.0/>.

© The Author(s) 2024